

Surface geosciences (Hydrology – Hydrogeology)
Effects of rock fragments on water movement and solute transport in a Loess Plateau soil

Zhou Beibei^{a,c}, Shao Ming'an^{a,*}, Shao Hongbo^{a,b,d}

^a State Key Laboratory of Soil Erosion and Dryland Farming on the Loess Plateau, Institute of Soil and Water Conservation, Chinese Academy of Science and Ministry of Water Resources, Northwest A & F University, 712100 Yangling, China

^b Shandong Key Laboratory of Eco-environmental Science for the Yellow River Delta, 256603 Binzhou, China

^c College of Resources and Environment, Northwest A & F University, 712100 Yangling, China

^d Institute of Life Sciences, Qingdao University of Science & Technology, 266042 Qingdao, China

Received 16 June 2008; accepted after revision 19 March 2009

Presented by Ghislain de Marsily

Abstract

Calcium carbonate concretions are present in the soil of the Loess Plateau as a result of pedogenesis. The presence of these small rock fragments can have a great impact on soil bulk density, structure and water storage properties, as well as on soil water movement and solute transport processes. We studied the effects of different gravimetric rock fragment contents in a soil (R_w) (0, 10, 20, 30, 40, 50, and 60%) on infiltration, saturated hydraulic conductivity (K_s) and solute transport. Both infiltration rates and the saturated hydraulic conductivity initially decreased with increasing rock fragment content to minimum values for $R_w = 40\%$, and then increased. The Peck–Watson and Bouwer–Rice equations predicted K_s for low rock fragment contents but failed to forecast the observed trends. Cumulative infiltration over time was described well by a power function. Solute transport processes, determined using CaCl_2 as a tracer, were accurately described by both the convection–dispersion equation (CDE) and the two-region model (T-R) although the T-R model fitted the experimental data a little better than the CDE, which is possibly more convenient to use. When R_w was about 40% solute transport parameters indicated that relatively more advection occurred in this mixture where immobile regions occupied the greatest proportion of the columns. *To cite this article: Z. Beibei et al., C. R. Geoscience 341 (2009).*

© 2009 Académie des sciences. Published by Elsevier Masson SAS. All rights reserved.

Résumé

Effets de la présence de fragments de roche sur le mouvement de l'eau et des solutés dans les sols loessiques du Plateau chinois. On observe la présence de concrétions carbonatées d'origine pédogénétique dans les sols de Plateau Loessique chinois. La présence de ces petits fragments de roche peut avoir des effets importants sur la densité apparente du sol, sa structure et ses propriétés de stockage de l'eau, ainsi que sur les mécanismes de transfert de l'eau et des solutés. Nous avons étudié l'influence de proportions pondérales R_w variables de fragments de roche dans un sol (0, 10, 20, 30, 40, 50, et 60 %) sur l'infiltration, la conductivité hydraulique à saturation K_s et le transport de solutés. Le taux d'infiltration et la conductivité hydraulique à saturation décroissent initialement avec la croissance de la teneur en fragments, jusqu'à des valeurs minima obtenues pour un taux de 40 %, puis recroissent. Les équations de Peck–Watson et Bouwer–Rice donnent une bonne prédiction de K_s pour les teneurs faibles en fragments de roche, mais sont incapables de prédire les tendances observées. L'infiltration cumulée est bien décrite par une fonction

* Corresponding author.

E-mail addresses: mashao@ms.iswc.ac.cn (S. Ming'an), shaohongbochu@126.com (S. Hongbo).

puissance. Les mécanismes de transport de solutés, étudiés par des traçages avec du CaCl_2 , sont bien reproduits par l'équation de convection–dispersion (CDE) ou par le modèle à deux régions (TR) ; ce modèle TR cale un peu mieux les données expérimentales que le modèle CDE, mais ce dernier est cependant plus facile à utiliser. Pour une teneur en fragments de roche R_w de l'ordre de 40 %, les paramètres de transport de soluté calés indiquent que l'advection est relativement plus importante dans le mélange, quand les régions à eau immobile occupent la proportion la plus grande de la colonne d'essai. **Pour citer cet article :** Z. Beibei et al., C. R. Geoscience 341 (2009).

© 2009 Académie des sciences. Publié par Elsevier Masson SAS. Tous droits réservés.

Keywords: Rock fragment content; Cumulative infiltration; Saturated hydraulic conductivity; Solute transport; Loess Plateau; China

Mots clés : Teneur en fragments de roche ; Infiltration cumulée ; Conductivité hydraulique saturée ; Transport de soluté ; Plateau loessique ; Chine

1. Introduction

Soil water hydrological processes control infiltration and surface runoff, and also the transport of pollutants, such as pesticides from agricultural land, either in overland flow or in percolating water that may enter the ground water [2,9,16]. Concerns about these processes and their consequences have motivated numerous experiments and theoretical studies relating soil properties to soil water movement and chemical transport.

Rock fragments are often present in soil as a result of soil forming processes and human activity. Rock fragments in the soil may influence water movement and solute transport by affecting the soil structure and the tortuosity of water flow paths, which may make water movement and solute transport more complex than in a stone-less soil [16,30]. Moreover, with increasing rock fragment content, the effects may become more significant. Since rock fragments in the soil can affect water movement and solute transport, they can in turn influence land use and site productivity [7,19,21]. Since the 1950s, scientists have studied the effect of rock fragments on several soil physical processes. Corey and Kemper [7] studied the reduction in evaporation rate attributable to rock fragments covering the soil surface and noted that, as with other mulch materials, they had the greatest inhibiting effect upon evaporation during the first few days after a rainfall event [7]. The effects of rock fragment cover in both increasing and decreasing infiltration were discussed in detail by Brakensiek and Rawls [4]. Valentin [28] studied the influence of rock fragments on surface sealing and concluded that relationships between sealing and rock fragments depended upon the pedoclimatic conditions [28]. Most studies, however, focused on the effect of the cover percentage of rock fragments on surface hydrological processes [18,19] whereas fewer have considered the effects of rock fragments in the soils on water movement and solute transport processes.

A particular characteristic of the soils of the Loess Plateau is that they are formed from loess deposits that have a high calcium carbonate content [26]. The source of these carbonates is both detrital, deposited following eolian transportation by monsoon winds, and authigenic [14]. Calcium carbonate concretions, resulting from pedogenesis, are often the main representatives of the authigenic carbonates and soils containing them are widespread [12]. The concretions form as a result of dissolution of calcium minerals in the presence of carbonic acid formed during the wet and humid weather of the summer and autumn from plant residues. The dissolved minerals are leached by percolating rainwater to lower depths where they are concentrated, coalesce, and dry out to form the calcium carbonate concretions. Processes such as uplifting and cultivation have subsequently redistributed these concretions, or rock fragments, within the upper soil profile where they can influence water movement and solute transport.

In this study, we determined water movement and solute transport processes through columns of disturbed soil samples containing rock fragments. The objective was to assess the effect of various rock fragment contents on soil water infiltration rates over time, the saturated hydraulic conductivity (K_s) and the solute transport process. The experimental data were also compared with existing models for K_s and solute transport in order to test their effectiveness in predicting these properties for a soil from the Loess Plateau containing rock fragments.

2. Material and methods

Samples of the A-horizon (10–30 cm depth) of a silty clay loam semi-luvisol (Chinese genetic soil classification system) [15] were collected at Xibo Village, Yangling District, Shaanxi Province, on the Loess Plateau, China. The soil samples were air-dried and the rock fragments (> 2 mm) were then separated from the

Table 1

Selected properties of the silty clay loam soil (International soil science society textural class).

Tableau 1

Quelques propriétés du limon argilo-silteux (classes de texture de la Société Internationale des Sciences du Sol).

Saturated water content ($\text{m}^3 \text{m}^{-3}$)	Sand content (kg kg^{-1})	Silt content (kg kg^{-1})	Clay content (kg kg^{-1})	Organic matter (kg kg^{-1})	Cation exchange capacity cmol kg^{-1}	Exchangeable sodium percentage (%)
0.235	0.263	0.482	0.364	0.015	14.6	0.3

finer soil ($< 2 \text{ mm}$) by sieving. The rock fragments were further sieved to obtain a fraction with an equivalent diameter of 10–30 mm. Selected soil properties are shown in Table 1; the particle size analysis was determined by sieving and the pipette method; organic matter was determined by potassium dichromate titration; cation exchange capacity was determined by barium chloride exchange; exchangeable sodium percentage was determined by ammonium acetate exchange [15]. The rock fragments were mainly composed of CaCO_3 ($> 90\%$) and had a saturated water content of $0.072 \text{ m}^3 \text{m}^{-3}$.

Air-dried fine soil samples ($< 2 \text{ mm}$) were mixed well with the rock fragments (10–30 mm) to give seven different gravimetric contents (0, 10, 20, 30, 40, 50, and 60%). The soil–rock fragment mixtures were then uniformly packed into acrylic plastic columns (height 50 cm, inner diameter 20 cm), the perforated bases of which were covered by a coarse filter paper (Fig. 1), to obtain a bulk density of 1.4 g cm^{-3} . The initial moisture contents of the fine soil and of the rock fragments were $0.012 \text{ m}^3 \text{m}^{-3}$ and $0.0048 \text{ m}^3 \text{m}^{-3}$, respectively. The surfaces of the soil mixtures were covered with a circle of filter paper to reduce disturbance from inflowing solutions.

Flow experiments were carried out by rapidly establishing and then maintaining a constant 4.5 cm head of deionized water on the surface of the soil using a Mariotte bottle (Fig. 1). The cumulative infiltration rate was initially determined from the volume of water supplied from the Mariotte bottle measured at timed intervals. After the wetting front had reached the base of the soil column the effluent was collected every 30 min and the volume measured until the flow rate became constant. The soil columns were then left to saturate for at least 24 h.

The distilled water in the Mariotte bottle was replaced with $0.15 \text{ mol L}^{-1} \text{ CaCl}_2$ solution, acting as a tracer, and the flow was resumed while maintaining a constant water head of 4.5 cm. The effluent was collected continuously in 150 ml volumetric flasks over timed intervals. The effluent samples were then titrated with silver chloride solution to determine the

Cl^- concentrations until they attained a stable level, close to 0.15 mol L^{-1} .

The experiments were carried out in three replications in a laboratory where the average temperature was $19 \pm 3 \text{ }^\circ\text{C}$. Relative humidity was not controlled but remained at $40 \pm 10\%$.

The saturated hydraulic conductivity of the soil–rock fragment mixtures ($K_s, \text{L T}^{-1}$) was calculated from the infiltration data using Darcy's law [20]:

$$K_s = \frac{QL}{A\Delta P} \quad (1)$$

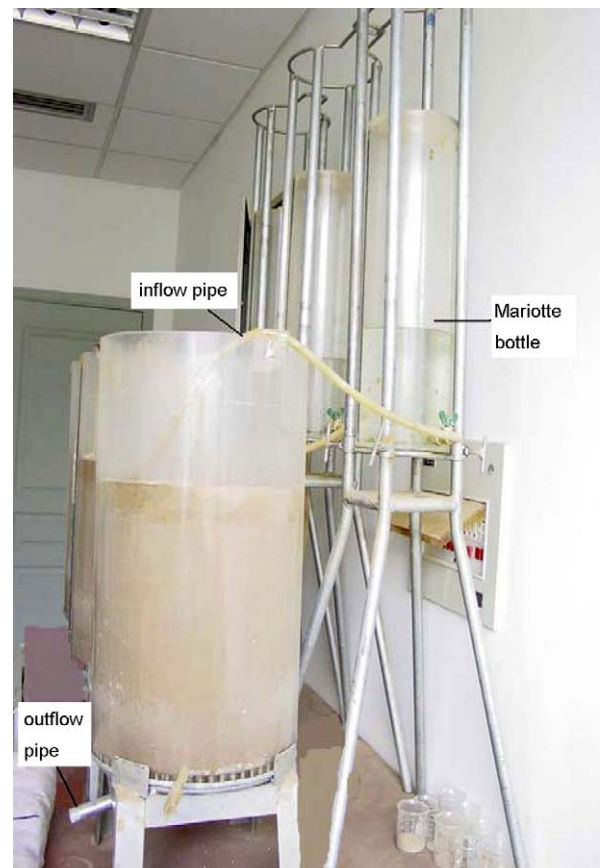


Fig. 1. Experimental setup for water flow and solute transport study.

Fig. 1. Dispositif expérimental d'étude de l'écoulement de l'eau et du transport de soluté.

where, Q is the volume of water flow per unit time ($L^3 T^{-1}$); L is the length of the soil column (L); A is the area of the soil column (L^2); ΔP is the hydrostatic pressure difference (L). The uniform mixing of the rock fragments with the fine soil was considered to satisfy the assumption made for the correct application of Darcy’s law that the medium through which the water flows should be homogeneous.

We wanted to compare our measured K_s values with those predicted by models devised for stony soils although literature on the hydraulic properties of such soils is limited. Peck and Watson [18] used a heat flow analogy for a medium in which there were spherical inclusions that were noninteractive to derive the following equation for the ratio of the field, or bulk, soil saturated hydraulic conductivity, K_b , to the fine-soil fraction saturated conductivity, K_s :

$$\frac{K_b}{K_s} = \frac{2(1 - R_v)}{2 + R_v} \quad (2)$$

where, R_v is the volumetric rock fragment content ($L^3 L^{-3}$).

Brakensiek and Rawls [8] pointed out that Eq. (2) was over-simplified and inaccurate. Bouwer and Rice (1984) used data from laboratory studies on sand-gravel mixtures to establish an expression that used void ratios [3]:

$$\frac{K_s}{K_b} = \frac{e_s}{e_b} \quad (3)$$

where, e_b and e_s are the void ratios for the bulk soil and fine soil fractions, respectively.

Therefore, in order to further discuss the effect of rock fragment contents on K_s , we calculated K_s using Eqs. (2) and (3) and then compared those theoretical solutions with our experimentally determined K_s values.

The experimental data of the solute transport were analyzed using two transport models, described below, that were fitted to the data using an iteration technique based on achieving the lowest sum of squares residual value (SSQ).

Model 1: The simplified convection–dispersion equation (CDE) [13], given by:

$$R \frac{\partial C}{\partial t} = D \frac{\partial^2 C}{\partial x^2} + \mu \frac{\partial C}{\partial x} \quad (4)$$

where R is the retardation factor (in our case, $R = 1$ because we used a conservative tracer); C is the concentration of solute in the liquid phase, ($M L^{-3}$); t is the

flow time, (T); D is the dispersion coefficient, ($L^2 T^{-1}$); μ is the pore water velocity, ($L T^{-1}$); and x , is the flow distance (L).

Model 2: The two-region model (T-R) is given by [11]:

$$\theta_m \frac{\partial C_m}{\partial t} + \theta_{im} \frac{\partial C_{im}}{\partial t} = \theta_m D \frac{\partial^2 C_m}{\partial x^2} - \mu_m \theta_m \frac{\partial C_m}{\partial x} \quad (5)$$

$$\theta_{im} \frac{\partial C_{im}}{\partial t} = \omega (C_m - C_{im}) \quad (6)$$

$$\theta = \theta_m + \theta_{im} \quad (7)$$

where θ_m is the volumetric water content in the mobile region, ($L^3 L^{-3}$), θ_{im} is the volumetric water content in the immobile region, ($L^3 L^{-3}$); C_m is the concentration in the mobile region, ($M L^{-3}$); C_{im} is the concentration in the immobile region, ($M L^{-3}$); D is the dispersion coefficient, ($L^2 T^{-1}$); μ_m is the pore water velocity in the mobile region, ($L T^{-1}$); t is the flow time, (T); x is the flow distance, (L); and ω is the mass transfer coefficient, (T^{-1}).

By taking the effluent concentration to be the flux-averaged concentration of the soil column, the initial and boundary conditions for this study can be assumed to be:

$$C_i = 0; \quad 0 < x < l \quad t = 0 \quad (8)$$

$${}_i C_0 = -D_i \frac{\partial C_i}{\partial x} + {}_i C_i; \quad x = 0, t > 0 \quad (9)$$

$$\frac{\partial C_i}{\partial x} = 0; \quad x = l, t > 0 \quad (10)$$

where C_i is the initial concentration in the mobile region, ${}_i$ is the pore water velocity in the mobile region, C_0 is the initial concentration in the whole soil column, D_i is the dispersion coefficient of the mobile region, l is the length of the soil column, and t is the flow time. The analytical solutions for the two models are found in van Genuchten [10]. These were used in conjunction with the nonlinear least-square curve-fitting program of van Genuchten [10] to estimate the unknown parameters in the two models from our observed effluent data.

Using the derived values of the dispersion coefficient (D or D_i) from each of the fitted solute transport models, we also calculated the dispersivity, λ , (L) and the Peclet number, Pe , defined by the following equations:

$$\lambda = \frac{D}{\mu} \quad (11)$$

$$Pe = \frac{l\mu}{D} = \frac{l}{\lambda} \quad (12)$$

3. Results and discussion

3.1. Infiltration

Fig. 2 presents the mean cumulative infiltration as a function of time for the rock fragment contents studied. Maximum values of the coefficients of variance for the cumulative infiltration occurring for a particular rock content were 2.4, 9.0, 6.5, 9.0, 8.8, 7.0 and 8.7% for the 0, 10, 20, 30, 40, 50, and 60% rock fragment contents, respectively. Smooth cumulative infiltration curves were obtained for all rock fragment contents, which follow a pattern similar to those typical for homogeneous soils without stones and indicate that the fine soil matrix was continuous in all cases. Cumulative infiltration increased at a significantly lesser rate when rock fragments were present than for the stoneless soil ($P < 0.05$) (Fig. 2). This indicates that the presence of rock fragments in the soil impeded infiltration. Additionally, during the early stage of the infiltration process, the effect of rock fragment content on cumulative infiltration was less noticeable but became so with time as the process of infiltration progressed. The effect of 10 and 20% rock fragment contents on cumulative infiltration was considerably smaller than that of higher rock fragment contents. Statistically, there was no significant difference between cumulative infiltration in the rock mixtures for R_w values of 10 and 20%, or for R_w values of 50 and 60%. We observed

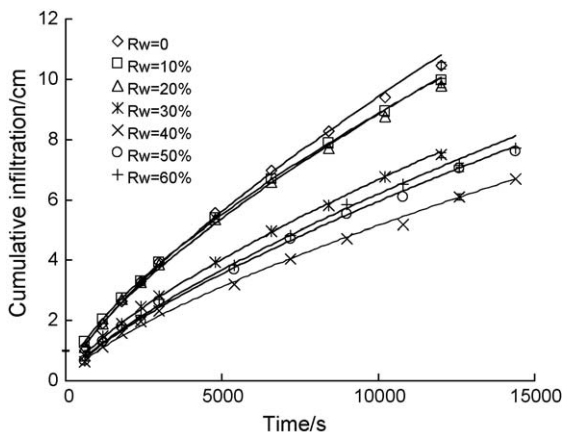


Fig. 2. Effect of rock fragment contents on cumulative infiltration over time. Symbols represent mean data points; solid lines are fitted curves using the Philip's infiltration equation; error bars for data points at about 12,000 s represent ± 1 standard deviation.

Fig. 2. Effet de la teneur en fragments de roche sur l'infiltration cumulée en fonction du temps. Les symboles représentent la moyenne des données expérimentales ; les lignes continues représentent le modèle d'infiltration de Philip calé sur ces données ; les barres d'erreur pour les mesures à 12 000 s. représentent \pm un écart-type.

the smallest rates of infiltration when R_w was 40% (Fig. 2).

In order to analyze the cumulative infiltration data, we fitted the experimental data with Philip's infiltration equation (Eq. [14]), the parameters of which are presented in Table 2:

$$I = St^{1/2} + At \quad (13)$$

where I is the cumulative infiltration (L), t is the time (T), and S is the sorptivity ($L T^{-1/2}$), A is the steady state infiltration rate ($L T^{-1}$).

Philip's infiltration equation considers both the downward movement of water, due to gravity, and advection due to matric forces. The coefficient of determination, R^2 , values were all above 0.99 indicating that the equation effectively described the relation between cumulative infiltration and time during the course of our experiment (Table 2). Both sorptivity and steady state infiltration were affected in a similar manner by increasing rock fragment contents (Table 2).

We regarded the rock fragments as impermeable. Thus, a main effect of the presence of the rock fragments is to reduce the area for water transmission and to increase the tortuosity of the water flow paths [6,17,27]. The values of sorptivity for rock fragment contents of 10 and 20% determined by Philip's equation are higher than that for the soil alone and may be an indication of this increased tortuosity. During the initial stage of the infiltration process, water movement into the dry soil is faster due to the presence of the matrix potential that exists at the wetting front between wet and dry soils. Since the presence of rock fragments might be expected to represent a discontinuity in the pore system, matrix potential might also be expected to decrease with increasing rock content. However, it appears from our data that, at a critical rock fragment content that appears to be about 40%, the rock fragments begin to contribute to a more continuous pore system. We attribute this to a greater degree of interconnection between the macropores that form around the fragments.

When the soil is wet, the increase in the volume occupied by the macropores associated with the increase in the rock fragment content may result in complex trends in water flow [22]. Continuous macropore systems can promote water flow whereas isolated macropores do not and, furthermore, are more likely to trap air, which interferes with water movement. Additionally, as the rock fragment content increases, there is a decrease in the effective porosity, i.e., the porosity where actual movement of water is possible and where isolated pores, for example, are excluded.

Table 2

Parameters for the Philip infiltration equation determined for soils with various rock fragment contents.

Tableau 2

Paramètres pour l'équation d'infiltration de Philip déterminés pour des sols à différentes teneurs en fragments de roche.

Parameter	Rock fragment content						
	0%	10%	20%	30%	40%	50%	60%
$S \text{ (cm/s}^{1/2}) \times 10^{-2}$	4.13 ± 0.02	4.76 ± 0.01	4.56 ± 0.02	3.13 ± 0.01	2.68 ± 0.01	2.81 ± 0.01	3.16 ± 0.04
$A \text{ (cm/s)} \times 10^{-2}$	0.05 ± 0.00	0.04 ± 0.00	0.04 ± 0.00	0.04 ± 0.00	0.02 ± 0.00	0.03 ± 0.00	0.03 ± 0.00
R^2	0.998	0.999	0.998	0.999	0.997	0.997	0.997

Note: R^2 is the coefficient of determination for the fit of $I = St^{1/2} + At$, where I is the cumulative infiltration, t is time, S is the sorptivity, and A is the steady state infiltration rate, with the experimental data.

Thus, we observe a decrease in infiltration due to decreasing effective porosity and the presence of isolated macropores as the rock fragment content increases. However, when the rock fragment content is about 40%, the macropore system appears to become more continuous to the extent that it facilitates water movement and, thus, infiltration subsequently increases with further increases in rock fragment content.

3.2. Saturated hydraulic conductivity (K_s)

Fig. 3 shows the effect of rock fragments on K_s and the comparisons of the experimental data with the calculated values determined by the Peck–Watson and Bouwer–Rice equations. The experimental values of K_s initially decreased with increasing rock fragment contents to a minimum value and then increased (Fig. 3). When $R_w = 40\%$, K_s had the smallest value. The trends in K_s values follow those observed for the cumulative infiltration and are explained in a similar manner. When the rock fragment contents are small, the

presence of nonporous fragments only reduces the available area for the flow and increases the tortuosity of the water flow. The increased tortuosity also results from the necessity for water to move laterally in order to wet the soil under the rock fragments. Although macropores are more likely to exist at the soil-to-rock interface, these are not continuous when the rock fragments are not in contact with each other, as would be the case in the mixtures with low rock fragment contents. Thus, increasing the rock fragment content initially increases the impedance of water flow and consequently K_s values become smaller. However, at a critical rock fragment content, which we observed to be about 40%, there are sufficient rock fragments in the soil to create more continuous macropores. Furthermore, fragment-to-fragment contact is more likely to create larger voids than those existing at the fragment-to-soil interfaces. Therefore, for rock fragment contents greater than this critical content, even though tortuosity increases, the creation of such larger and more continuous macropores appears to be beneficial for water flow and results in the observed increase in saturated hydraulic conductivity with further increases in rock fragment contents [8,21].

From Fig. 3 it can also be seen that the K_s values calculated by the Peck–Watson equation were consistently smaller than those predicted by the Bouwer–Rice equation, which was also found to be the case by Sauer and Logsdon [24]. Furthermore, neither equation correctly predicted the trend in the relation between K_s and rock fragment content although there were some coincidental agreements between the experimental data and the calculated values, notably for the two lower rock fragment contents. Zhou and Shao [29] similarly reported that the Peck–Watson and Bouwer–Rice equations were only valid for estimating K_s for soil containing small amounts of elliptical rock fragments and that, with increasing content of these elliptical rock fragments, both equations over-estimated the value of K_s . Bagarello et al. [1] pointed out that determining the

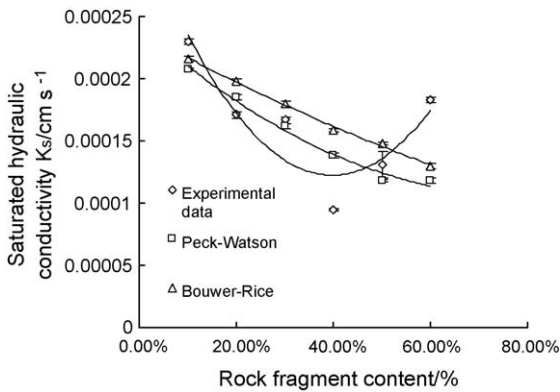


Fig. 3. Comparison of K_s determined experimentally and from equations proposed by Peck and Watson [18] and Bouwer and Rice [5]. Error bars represent ± 1 standard deviation.

Fig. 3. Comparaison de la perméabilité K_s déterminé expérimentalement et à partir des équations de Peck et Watson [18] et de Bower et Rice [5] ; les barres d'erreur représentent \pm un écart-type.

void ratio measurements used in the Bouwer–Rice equation are not necessary to predict K_b/K_s since the e_s/e_b ratio equals $1 - R_w$ and can thus be simply determined by the direct measurement of R_w [2]. Thus our results and the findings of these other studies suggest that the use of a simple experimental approach to determine the saturated hydraulic conductivity of a soil containing rock fragments can be advantageous in the absence of accurate models.

3.3. Solute transport

Fig. 4a–g presents the breakthrough curves of the 0.15 mol L^{-1} CaCl_2 solution used as a flow tracer for the soil samples with different rock fragment contents. The data in these figures showed that, even when the rock fragment content was as great as 60% (Fig. 4a–g), smooth breakthrough curves were obtained that followed a similar trend to those typical for a homogeneous soil without stones. Russo, experimenting on a soil containing 50–70% rock fragments by weight, similarly observed that the solute transport process in the stony soil was very similar to that in the homogeneous stoneless soil [23].

Our experimental data were fitted using both the CDE and the T-R. Fig. 4a–g indicates that the T-R model provided a slightly better fit to the data than the CDE, especially in its ability to describe the steep initial increases in relative concentration and the tailing phenomenon. From Fig. 4a–g, it can be seen that Cl^- was detected earliest in the effluent from soil–rock fragment mixtures when R_w was 60%, which was probably due to the greater preponderance of continuous macropores that facilitated rapid solute flow. The presence of Cl^- was detected latest in the effluent from soil–rock fragment mixtures when R_w was 40%, which was the critical content noted above as the level at which K_s was the lowest value while the presence of macropores was probably least beneficial because they did not yet form a continuous macropore system.

When R_w was 0%, breakthrough occurred in the shortest time in the soil columns while the longest time for breakthrough was observed when R_w was 40% (Fig. 4a–g). Comparing the various breakthrough curves in Fig. 4a–g, it can be seen that, when there were no rock fragments in the soil, Cl^- was present in the effluent in a relatively short time and also took a short time to break through. This can be attributed to the homogeneity of the pore system and the high K_s value. In contrast, when R_w was 60%, although Cl^- was present in the effluent in a relatively short time, it took a relatively long time for breakthrough to occur. The former can be attributed

to the rapid transport of solute through the macropore system while the latter results from the increased tortuosity, which led to the longer time required in order to saturate the zones with finer pores created below the rock fragments and the immobile regions. The longest time between the initial detection of Cl^- and breakthrough was observed when R_w was 50%.

Table 3 compares the two models describing solute transport. The SSQ values indicate that both models predicted values for relative concentrations of Cl^- that fitted the experimental data well. However, in general, the T-R model fits the experimental data slightly better than the CDE. This can be attributed to the greater number of parameters used in the T-R model than were used in the CDE that more accurately describe the solute transport processes.

Table 3 lists the Peclet number, Pe , and the dispersivity, λ , determined from the values of the dispersivity coefficients obtained by fitting either the CDE or the T-R model, and the mobile–immobile partition coefficient, β , and the mass transfer coefficient, ω , derived by the T-R model alone.

From Table 3, it can be seen that the values of the dispersivity, λ , when calculated by the CDE were about twice as great as those obtained with the T-R model and followed the same trend (Table 3). This can be attributed to the fact that the CDE combines the effect of solute exchange between the mobile and immobile regions into one term, the equivalent dispersion coefficient, while the processes of hydrodynamic dispersion and diffusional exchange are treated separately by the T-R model [29]. Thus, the value for dispersivity in the T-R model accounts for only part of the dispersion phenomenon, the other part being accounted for by the exchange coefficient, and is therefore always smaller than the dispersivity value obtained by the CDE. The values of the dispersivity are an indication of the distance travelled by the solute. Thus, the value was small when the path taken by the solute in the column was less tortuous as was the case for the stoneless soil, the most homogeneous medium studied. It was also relatively small when the rock fragment content was 40% with values comparable to those of the stoneless soil (Table 3). It appears that the solute was totally excluded from regions within that soil–rock fragment matrix and was confined to direct, almost vertical, pathways. Since such pathways would have only existed in a fraction of the volume occupied by the medium, this explanation could also account for the low K_s value observed.

The Pe values of the soil column varied with the various rock fragment contents (Table 3). When the R_w reached 40%, the value of the Pe was the largest of all

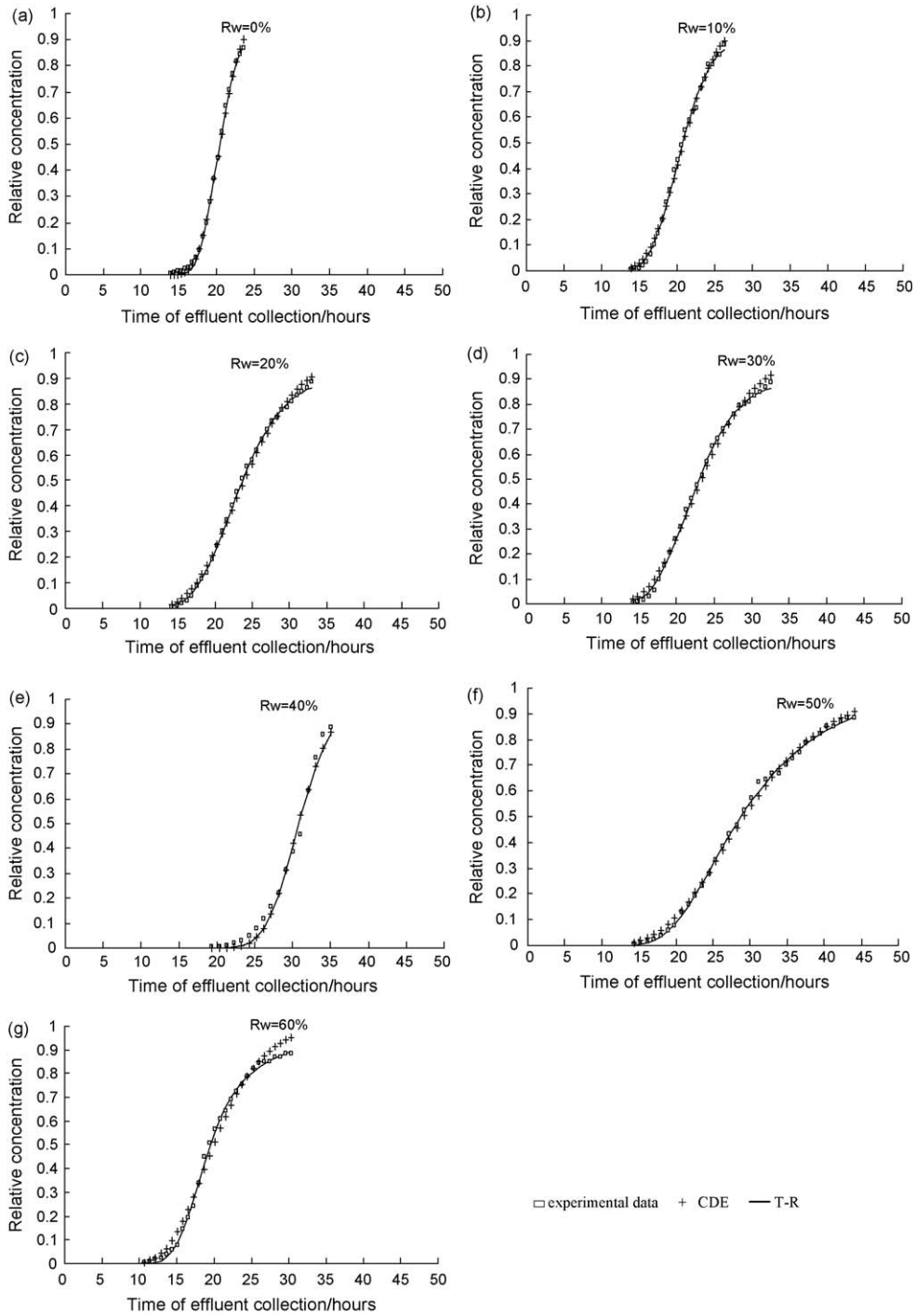


Fig. 4. (a–g) Comparison of the ratio of concentrations of Cl^- in the effluent to that in the leaching solution when determined experimentally and when derived by the classic diffusion equation (CDE) or the two-region model (T-R).

Fig. 4. (a–g) Comparaison du rapport de la concentration en Cl^- dans l’effluent à celle de la solution entrante, valeur expérimentale et celles obtenues avec le modèle CDE classique ou avec le modèle T-R à deux régions.

Table 3

Values of the Peclet number, Pe, dispersivity, λ , the mobile-immobile partition coefficient, β , and the mass transfer coefficient, ω , when derived by either the convection dispersion equation (CDE) or the two region model (T-R).

Tableau 3

Valeurs du nombre de Péclet, Pe, de la dispersivité, λ , du coefficient de partage mobile-immobile β , et du coefficient de transfert de masse ω , obtenus à partir de l'équation de convection–dispersion CDE ou du modèle à deux régions T-R.

R_w (%)	SSQ		Pe		λ		β		ω	
	CDE	T-R	CDE	T-R	CDE	T-R	CDE	T-R	CDE	T-R
0	3.53E-03	2.19E-03	160.64	210.49	0.42	0.25	-	0.72	-	0.065
10	1.04E-02	6.48E-03	61.73	71.70	1.02	0.59	-	0.67	-	0.099
20	1.15E-02	2.44E-03	33.02	39.99	1.85	0.94	-	0.61	-	0.13
30	1.59E-02	3.32E-03	33.05	43.25	1.62	0.84	-	0.66	-	0.15
40	1.72E-02	3.13E-02	150.61	172.70	0.48	0.27	-	0.88	-	0.01
50	1.11E-02	5.32E-03	19.79	20.22	2.77	1.70	-	0.80	-	0.15
60	3.47E-02	4.40E-03	29.89	27.60	1.77	0.63	-	0.86	-	0.46

Note: SSQ is the sum of squares residual.

the mixtures and comparable to that of the stoneless soil. The values of the Peclet number determined using values for the dispersion coefficient derived from the CDE and the T-R model generally followed the same trend for both models, although those predicted by the former are typically lower than those obtained by the latter, and reflect the inverse relationship between the Peclet number and the dispersivity (Table 3). The Peclet number is a measure of the movement of the solute by mass flow moving vertically in the columns compared to dispersion that involves advective movement and higher numbers indicate that the latter process dominates. Thus, in all the columns, diffusive flow was the dominant component of solute transport but was especially so for those that contained stone-free soil and the soil with an R_w of 40%. This indicates that there was minimal impedance to sideways movement in the homogeneous stoneless soil, as expected, and also that in the $R_w = 40\%$ mixture, which suggests that possibly the macropores present in this mixture may have been dominated by horizontally oriented larger pores. It appears that even low rock fragment contents impeded diffusive flow considerably and that increases in the rock fragment content above $R_w = 40\%$ also impeded diffusive flow (Table 3).

The mobile–immobile partition coefficient, β , of the T-R model represents the fraction of solute present in the mobile region under equilibrium conditions [25]. Table 3 showed that this fraction in mobile water initially declined with increasing rock content but values did not vary greatly for contents between 10 and 30%. The fraction became significantly larger when R_w was 40% but again did not vary greatly when R_w was between 40 and 60%. This suggests that, once the rock fragment content volume reaches the critical level of about 40%, which corresponded to the creation of a

significant macropore system, the volume of the column occupied by the immobile regions increased significantly and was not subsequently greatly affected by the further development of that system. These immobile regions might usually be expected to result in increased advection of solute, which was indicated by the highest Peclet number derived for $R_w = 40\%$.

The mass transfer coefficient, ω , of the T-R model is conceptually related to the dispersivity, λ . Thus, in general, the trends in ω are a reflection of those seen in λ although the changes in magnitude are not directly proportional (Table 3).

4. Conclusions

This study shows that the presence of rock fragments in soil affects the infiltration process but that the overall continuity of the medium was sufficient to result in smooth cumulative infiltration curves, described well by a power function, even when 60% consisted of rock fragments by weight. Infiltration rates over time and the K_s values first decreased with increasing rock fragment content to an observed minimum, when the content was 40%, and then increased. Both the Peck–Watson equation and Bouwer–Rice equation provided estimates of K_s that were close to the experimental data when the rock fragment content was less than 20% but failed to predict the trends observed experimentally for higher contents. The increases in K_s and infiltration above rock fragment contents of about 40% were ascribed to the development of a more continuous macropore system.

The solute transport experiment confirmed the overall continuity of the medium even for the most heterogeneous soil–rock mixture as indicated by the smooth breakthrough curves. For larger rock fragment contents, breakthrough curves were described slightly

better by the T-R model than by the CDE. However, the simpler CDE proved to be sufficiently accurate for simulating solute movement in the soil containing rock fragments. The Peclet number was largest when R_w was 40% corresponding to the lowest observed K_s , indicating that advection occurred at the greatest degree in this mixture of those studied. The mobile-immobile partition coefficient, β , values were similar when the rock fragment contents were either below or were above or equal to 40% but differed significantly around this critical content.

This study provides evidence that can enhance the understanding of the role of rock fragments in water movement and solute transport in soils on the Loess Plateau. Knowledge of the effect of the infiltration and solute transport processes in soils in relation with the content of rock fragments can facilitate management strategies that can reduce runoff and associated soil erosion, and/or nutrient losses on the Loess Plateau. Further in depth and systematic research is required as the distribution and range of the rock fragments in soils is more complex in nature and results need to be transferred to the field.

Acknowledgements

The work in this paper is supported by National Natural Science Foundation of China (50479063, 40025106, 90102012, 90502006), Shao Ming-An's Changjiang Scholar Innovation Team Projects of Education Ministry of China and Innovation Team Group Projects of Northwest A&F University, the International Cooperative Partner Plan of Chinese Academy of Sciences, and One-hundred-Talent Plan of Chinese Academy of Sciences. The authors thank the four reviewers for the constructive comments on the manuscript, especially Professor G. de Marsily (at University Paris VI, Member, French Academy of Sciences) for the excellent editing and correcting of the revision. We also extended our sincere thanks to Assistant Editor, Marina Jimenez for the kind suggestions and guidance.

References

- [1] V. Bagarello, D.E. Elrick, M. Iovino, A. Sgroi, A laboratory analysis of falling head infiltration procedures for estimating the hydraulic conductivity of soils, *Geoderma* 135 (2006) 322–334.
- [2] V. Bagarello, M. Iovino, Comments on “Predicting the effect of rock fragments on saturated soil hydraulic conductivity”, *Soil Sci. Soc. Am. J.* 71 (2007) 1584.
- [3] H. Bouwer, R.C. Rice, Hydraulic properties of stony vadose zones, *Soil Sci. Soc. Am. Proc.* 48 (1984) 736–740.
- [4] D.L. Brakensiek, W.J. Rawls, Soil containing rock fragments: effects on infiltration, *Catena* 23 (1994) 99–110.
- [5] B. Buchier, C. Hinz, M. Flury, Heterogeneous flow and solute transport in an unsaturated stony soil monolith, *Soil. Sci. Soc. Am. Proc.* 59 (1995) 14–21.
- [6] S.W. Childs, A.L. Flint, Physical properties of forest soil containing rock fragments, in : S.P. Gessel, D.S. Lacate, G.F. Weetman, R.F. Powers (Eds.), *Sustained Productivity of Forest Soils*, University of British Columbia, Faculty of Forestry, Vancouver, BC, 1990, pp. 95–121.
- [7] A.T. Corey, W.D. Kemper, Conservation of Soil Water by Gravel Mulches, *Hydrology Papers Volume 30*, Colorado State University, Fort Collins, CO, 1968, pp. 1–24.
- [8] I. Cousin, B. Nicoullaud, C. Coutadeur, Influence of rock fragments on the water retention and water percolation in a calcareous soil, *Catena* 53 (2003) 97–114.
- [9] M. Fournier, N. Massei, M. Bakalowicz, J.P. Dupont, Use of univariate clustering to identify transport modalities in karst aquifers, *C.R. Geoscience* 339 (2007) 622–631.
- [10] M.T. van Genuchten, Non-equilibrium transport parameters from miscible displacement experiments, Research report, no.119. U.S. Salinity Laboratory, Riverside, CA, 1981.
- [11] M.Th. van Genuchten, R.J. Wagenet, Two-site/two-region models for pesticide transport and degradation: theoretical development and analytical solutions, *Soil Sci. Soc. Am. J.* 53 (1989) 1303–1310.
- [12] J.M. Han, E. Keppens, T.S. Liu, Stable isotope composition of the carbonate concretion in Loess and climate change, *Quatern. Int.* 37 (1997) 37–43.
- [13] L. Lapidus, N.R. Amundson, Mathematics of adsorption in beds, V. Effect of Intra-particles Diffusion in Flow System in Fixed Beds, *J. Phys. Chem.* 56 (1952) 683–688.
- [14] X.M. Liu, T.S. Liu, J. Shaw, The magnetic characteristic of Chinese Loess and paleoclimatic implication, *Quatern. Res.* 3 (1993) 282–287 (in Chinese).
- [15] R.K. Iv, Nanjing Agricultural University, *Soil Agrichemical Analysis*, Agriculture Press, Beijing, China, 1992, pp. 37–103 (in Chinese).
- [16] D.H. Ma, M.A. Shao, Simulating infiltration in stony soil with a dual-porosity model, *Eur. J. Soil Sci.* 59 (2008) 950–959.
- [17] G.R. Mehuys, L.H. Letey, I.V. Weeks, Temperature distributions under stones submitted to a diurnal heat wave, *Soil Sci.* 120 (1975) 437–441.
- [18] A.J. Peck, J.D. Watson, Hydraulic conductivity and flow in non-uniform soil, Workshop on soil physics and field heterogeneity, CSIRO Div. Environ. Mech., Canberra, 1979.
- [19] J. Poesen, H. Lavee, Rock fragments in top soils: significance and processes, *Catena* 23 (1994) 1–28.
- [20] Y.D. Qing, *Soil Physics*, Higher Education Press, Beijing, China, 2003, 39p (in Chinese).
- [21] I. Ravina, J. Magier, Hydraulic conductivity and water retention of clay soils containing rock fragments, *Soil Sci. Soc. Am. J.* 48 (1984) 736–740.
- [22] W.J. Rawls, Estimating soil bulk density from particle size analysis and organic matter content, *Soil Sci.* 135 (1983) 123–125.
- [23] D.L. Russo, Characteristics of a stony desert soil, *Soil. Sci. Soc. Am. J.* 47 (1983) 431–438.
- [24] T.J. Sauer, S.D. Logsdon, Hydraulic and physical properties of stone soils in a small watershed, *Soil Sci. Soc. Am. J.* 66 (2002) 1947–1956.

- [25] R. Schulin, M.T. van Genuchten, An experimental study of solute transport in a stony field soil, *Water Resour. Res.* 23 (1987) 1785–1794.
- [26] K.L. Tang, X.B. He, Re-discussion on Loess-Paleosol evolution and climate change on the Loess Plateau during the Holocene, *Quatern. Sci* 24 (2004) 129–139 (in Chinese).
- [27] J.S. Thomas, D.L. Sally, Hydraulic and physical properties of stony soils in a small watershed, *Soil Sci. Soc. Am. J.* 66 (2002) 1947–1956.
- [28] C. Valentin, Surface sealing as affected by various rock fragment covers in West Africa, *Catena* 23 (1994) 87–97.
- [29] B.B. Zhou, M.A. Shao, Study on saturated hydraulic conductivity of soil stone mixtures, *J. Soil Water Conser.* 20 (2006) 62–66 (in Chinese).
- [30] B.B. Zhou, M.A. Shao, Effect of different rock fragments contents and sizes on infiltration, *Acta Pedol. Sin.* 44 (2007) 801–1801.